

Accepted Manuscript

A finite element based approach for fatigue life prediction of headed shear studs

Md. Manik Mia, Anjan K. Bhowmick



PII: S2352-0124(19)30001-3
DOI: <https://doi.org/10.1016/j.istruc.2019.01.001>
Reference: ISTRUC 379
To appear in: *Structures*
Received date: 6 September 2018
Revised date: 27 December 2018
Accepted date: 3 January 2019

Please cite this article as: Md. Manik Mia, Anjan K. Bhowmick , A finite element based approach for fatigue life prediction of headed shear studs. Istruc (2019), <https://doi.org/10.1016/j.istruc.2019.01.001>

This is a PDF file of an unedited manuscript that has been accepted for publication. As a service to our customers we are providing this early version of the manuscript. The manuscript will undergo copyediting, typesetting, and review of the resulting proof before it is published in its final form. Please note that during the production process errors may be discovered which could affect the content, and all legal disclaimers that apply to the journal pertain.

A finite element based approach for fatigue life prediction of headed shear studs

Md. Manik Mia and Anjan K. Bhowmick

Department of Building, Civil and Environmental Engineering, Concordia University,
Montreal, Quebec, Canada

Abstract: Steel shear studs in bridges are subjected to rapidly fluctuating stresses causing fatigue failure. Research on fatigue of shear studs mainly focused on tests. Both AASHTO and Canadian design curve for fatigue resistance of shear studs are based on the tests conducted in the mid 1960's by Slutter and Fisher. This paper presents a finite element based approach using push-out specimen for fatigue life estimation of headed shear stud connectors. Both crack initiation and crack propagation life are estimated and an excellent correlation is found when compared against test results. In addition, since a significant amount of push-out tests data on headed shear studs are now available, this paper evaluates the fatigue design curves of different standards, with special focus given to evaluation of the value of constant amplitude fatigue limit (CAFL) given in the current AASHTO and Canadian code (CSA S6-14). The regression analysis also shows that the current fatigue curves in different codes can be used for shear studs as large as 31.8 mm. Thus, restriction of use of studs larger than 25 mm (1 inch) in different bridge codes (CSA S6, Eurocode 4, and AASHTO) can be waived.

Keywords: Fatigue-life; crack initiation life; crack propagation life; push-out test; shear stud

1. Introduction

Headed shear studs are used worldwide in steel-concrete composite bridges and these shear connectors are welded on top of steel beam. Their primary purpose is to prevent horizontal movement and separation between steel beam and concrete slab, which allows them to act as one unit. One of the major drawbacks of headed shear stud connectors is that it is very sensitive to fatigue and care must be taken if used in fatigue prone sites. Repeated or fluctuating stress can initiate micro-cracks in materials which may propagate with the continued application of cyclic stress. This process is known as fatigue. In bridges, fatigue failure can be dangerous since it occurs suddenly without significant prior deformations. Thus, the fatigue resistance of shear studs in composite beams is important for the safe of whole structure and needs to be well investigated.

Bridge Design Codes (CSA S6-14 [1]; ASSHTO 2014 [2]; Eurocode 4 [3]) provide design guidelines for headed shear stud to meet both ultimate limit state (ULS) and fatigue limit state (FLS). In all the codes, to satisfy fatigue requirements at the FLS, designers will have to keep the stress levels below an empirically determined threshold for a given number of load cycles. Previous edition of CSA S6 (CSA S6-06 [4]) had exactly same equations as AASHTO for design of headed shear studs subjected to fatigue loading. These equations were based on fitting a curve through the push-out test data of Slutter and Fisher [5]. The test performed by Slutter and Fisher [5] in Leigh University is considered as one of the major works in fatigue problems of shear studs in steel-concrete composite beam. Slutter and Fisher [5] tested 44 samples containing 19 mm and 22 mm studs under constant amplitude stress cycles ranging from 55 MPa to 138 MPa and it was reported that stress

range rather than maximum stress is the important factor for fatigue life of shear studs. The effect of minimum stress was found to be significant only in case of stress reversals.

Most of the research on shear stud focussed mainly on medium and small diameter studs. Thus, design codes have restrictions for selection of shear studs. In CSA S6-14, the use of studs with a diameter greater than 25 mm (1 inch) is not permitted. AASHTO does not recommend use of shear stud diameter larger than 1¼". According to Eurocode 4, shear stud should have diameter between 16 mm and 25 mm and the tensile strength of the stud should be less than 500 MPa. Yet, often it becomes necessary to use shear studs with large diameter and higher strength in construction. Another important consideration in design of shear studs is the strength of the concrete deck. Current fatigue equations in design codes are based on push-out tests of shear studs embedded in light weight and normal weight concrete. Shear studs now-a-days are widely used in composite girder bridges with high performance and ultra-high performance concrete decks with strengths significantly exceeding those of normal weight concrete. Thus, applicability of code equations and design curves for fatigue design of larger shear studs and fatigue design of studs embedded in high strength concrete needs to be studied. Fatigue resistance of shear stud is best determined through testing, which is very expensive and time consuming. It is often impractical, and sometimes impossible, to test full size structural components. Thus, analytical prediction models are often required as an alternative mean. A detailed finite element model of push out test has been developed using general purpose finite element software ABAQUS [6]. The FE model included both geometric and material nonlinearities. Using the developed model, a FE based approach for fatigue life estimation is proposed

using push-out specimen. A parametric study is then conducted using the validated FE model to investigate effects of different parameters, such as stud spacing and concrete compressive strength, on fatigue life of shear studs.

As stated earlier, the AASHTO design curve for fatigue resistance is based on the research conducted in the mid 1960's by Slutter and Fisher. However, a significant amount of push-out tests have been conducted to investigate the fatigue resistance of shear connectors since 1960's. Lee et al. [7] experimentally investigated the fatigue property of large diameter shear studs subjected to low cycle fatigue load. They pointed out that the fatigue strength of large studs was a little lower than that of normal studs. Mundie [8] performed twelve push-out tests and reported significant underestimation in fatigue life of shear studs by AASHTO. With large amount of push-out test data available fatigue design curves available in different bridge standards can be evaluated. This is done in this paper by conducting a regression analysis of available push-out test data. One important difference in fatigue design of shear stud between Eurocode and the North American bridge codes is that unlike European counterpart, where no constant amplitude fatigue limit (CAFL) is recommended, North American bridge codes recommend a CAFL value of 48 MPa. Constant amplitude fatigue limit/threshold is the stress range below which there will not be any fatigue failure and the stud is assumed to have an infinite fatigue life. In reality, however, the stresses a bridge experience over its design life are variable in amplitude. In both S6-14 and AASHTO, to ensure an infinite fatigue life for shear stud, the constant amplitude threshold is divided by 2 to obtain variable amplitude fatigue limit stress range. Assessment of the CAFL value provided in AASHTO and CSA S6 requires close

examination of test data of push-out specimens subjected to stress amplitude near the CAFL value. This paper also evaluates the constant amplitude fatigue limit (CAFL) given in current AASHTO and Canadian code.

2. Fatigue life prediction techniques

There are two basic approaches that are used to calculate total number of cycles a component can sustain before failure: use of $\Delta\sigma - N$ curves and fracture mechanics approach. In this paper, fracture mechanics approach is used to predict total fatigue life. In fracture mechanics approach, there are three stages of crack growth: crack initiation stage, stable crack propagation stage and unstable crack propagation stage. The total fatigue life is the sum of crack initiation and crack propagation life. Crack initiation life is calculated using empirical correlation approach and stable crack propagation life is calculated using linear elastic fracture mechanics (LEFM) approach. The strain-based method by Smith et al. [9], Eq. (1), is used in this study for calculating fatigue crack initiation life.

$$\frac{\Delta\varepsilon}{2} = \frac{(\sigma'_f)^2}{\sigma_{max}E} (N_{init})^{2b} + \frac{\sigma'_f \varepsilon'_f}{\sigma_{max}} (N_{init})^{b+c} \quad (1)$$

where $\frac{\Delta\varepsilon}{2}$ is the strain range, σ_{max} is the maximum local stress accounting for plasticity, E is the modulus of elasticity, σ'_f is fatigue strength coefficient, ε'_f is fatigue ductility coefficient, b and c are fatigue strength exponent and fatigue ductility exponent, respectively and N_{init} is the crack initiation life. The crack initiation life parameters are obtained from the research work of Josi and Grondin [10]. Once the crack is initiated, it starts to propagate with the subsequent load cycles. In this stage, crack front grows more and more until failure occurs. According to Paris [11], the logarithm of crack growth rate,

da/dN is proportional to logarithm of stress intensity factor range, ΔK and can be expressed as:

$$da/dN = C (\Delta K)^m \quad (2)$$

where C and m are material constants. It has been observed that crack does not propagate if stress intensity factor is less than a certain value known as threshold stress intensity factor range, ΔK_{th} . Following equation has been used in this paper to estimate crack propagation life:

$$N_{prop} = \int_{a_o}^{a_f} \frac{da}{C (\Delta K^m - \Delta K_{th}^m)} \quad (3)$$

where a_o and a_f are the initial and final crack sizes respectively. As per guidelines of ASTM standard [12], ΔK can be taken as $\Delta K = K_{max}$ if only tension portion of stress cycles are considered. From the research work of Fisher et al. [13] and Ibrahim et al. [14], it has been found that initial crack size is the most important factor in crack propagation life and final crack size is less significant. Ellyin [15] pointed out the restrictions to use LEFM approach in case of very small initial crack size and Chen et al. [16] suggested 1 to 5 mm as initial crack size. In this study, initial crack size of 1.0 mm was used and it gave an excellent correlation with test results.

3. Nonlinear finite element model of push-out test

A detailed nonlinear finite element model has been developed for simulating push-out test. The push-out specimen similar to those of Lee et al. [7] test was used in this study for fatigue life investigation and the essential components of push-out specimen were modeled with the help of general purpose finite element software ABAQUS [6].

3.1 Model geometry

For the detailed FE model, all the components of push-out specimen such as concrete slab, steel beam, shear stud and rebar were modeled. The thickness of steel beam and concrete slab were 14 mm and 200 mm respectively. Fig 1(a) presents the geometry of the push-out test by Lee et al. [7]. Due to the symmetry of push-out specimen, a quarter of the whole model shown in Fig. 1(b) was used. The headed shear stud is the most key element in push-out specimen. Two shear studs of 25 mm and 27 mm diameter were selected with weld collar height of 7 mm.

3.2 Contact and interaction

In order to simulate proper test condition, it is very important to use proper constraint between different parts of the push-out specimen in FE analysis. The nodes of the concrete slab and steel beam around the studs were constrained to the surfaces of shear studs by using tie constraint. In Abaqus, it is necessary to define master and slave surfaces. Shear studs were selected as master surface and concrete slab as slave. Surface-to-surface contact procedure was used in Abaqus/Explicit with normal behavior (“Hard” contact) and tangential behavior (“frictionless” formulation). A frictionless interaction was used between steel beam and concrete slab. Figure 2 shows the surfaces used for tie constraint definition. For this study, a displacement controlled procedure was followed. Downward displacement was applied to the top surface of the steel beam denoted as “Load surface” in Fig. 3. MPC constraint was used between load surface and the control point to ensure uniform distribution of load/displacement. ABAQUS allows to apply load on a surface uniformly through MPC constraint by connecting all the nodes lying on that surface to the constraint control point.

3.3 Boundary condition

Boundary conditions are very important for the simulation of experimental program and any inappropriate boundary conditions may cause completely different and wrong results. As shown in Fig. 4, X-axis symmetric boundary condition (BC) was applied to surface 1 and all the nodes lying in surface-1 were restricted from moving in the X direction and rotation about Y and Z axis were also restrained. The Z-axis symmetric BC was applied to the middle of the steel beam web and all the nodes in the middle of the steel beam web, designated as surface 2, were restrained in Z direction, as well as rotation about X and Y axis were also restrained. At the bottom surface of concrete slab, all translational and rotational movements were restrained.

3.4 FE mesh

To obtain accurate results from finite element analysis of the detailed model, three-dimensional solid element (hexahedral) was used to model the push-out components provided they are not distorted. Solid elements can be used for both linear and complex non-linear simulations involving contact, plasticity and large deformations. For concrete slab, steel beam and headed shear studs, three-dimensional eight-node element (C3D8R) was selected and T3D2 truss element with linear approximation of displacement was used for rebar. T3D2 element has two nodes and three translational degrees of freedom. Figure 5 presents FE meshes for the concrete slab, steel beam and shear stud with weld collar. A mesh convergence study was conducted to select the appropriate mesh size for the push-out model of Gattesco and Giuriani [17]. It was observed that the difference in results (test/predicted) for each shear stud was less than 1% when overall mesh size increased from

10 mm to 25 mm. Thus, to reduce the computation time, 25 mm mesh size was selected in this study.

3.5 Material properties

In this paper, the uniaxial stress-strain curve of concrete used in Eurocode, as shown in Fig. 6, was used with slight modifications. There are three parts in this stress-strain curve; in first part, stress increases linearly up to $0.4 f'_c$. The young's modulus is calculated based on the formula of CSA A23.3-14 [18]:

$$E_{concrete} = 4500\sqrt{f'_c} \quad (4)$$

where f'_c and $E_{concrete}$ are cylindrical compressive strength and modulus of concrete respectively. The second part of the curve is an ascending part up to $0.9 f'_c$ and the peak stress was used as $0.9 f'_c$, as suggested in CSA A23.3-14 [18]. The strain (ϵ_{c1}) related to $0.9 f'_c$ was taken as 0.0022 and Poisson's ratio of 0.2 was used for concrete. The third part of the curve is a descending part up to $r f'_c$, where the value of r is the reduction factor taken from the study of Ellobody et al. [19]. The ultimate strain ($\alpha\epsilon_{c1}$) of concrete was used as 0.0035, as suggested by CSA A23.3-14 [18]. For concrete in tension, the tensile stress is assumed to increase linearly until crack forms and f_t is calculated based on CSA A23.3-14 [18]:

$$f_t = 0.6\sqrt{f'_c} \quad (5)$$

where f_t and f'_c are in MPa. Finally, f_t , tensile stress decreases linearly to zero. The strain ($\beta\epsilon_t$) at zero tensile stress was taken as 0.005. Concrete damaged plasticity model available in ABAQUS was used in the definition of concrete material in FE model. In order to represent the inelastic behavior of concrete, yielding parts of the stress-strain curve of

concrete are used separately in this material model for compression and tension. Concrete damaged plasticity model assumes a non-associated potential plastic flow, and Drucker-Prager hyperbolic function was used in this study. The dilation angle was taken as 20° . The ratio of biaxial compressive strength to uniaxial compressive strength and eccentricity were taken as 1.16 and 0.10, respectively as suggested in ABAQUS.

For both structural and reinforcement steel, bi-linear stress-strain relationships were assumed representing a simple elastic-plastic model. Poisson's ratio was taken as 0.3 for structural and reinforcement steel material. The material properties used in the tests of Lee et al. [7] for structural and reinforcement steel and headed studs were used in the FE analysis.

The nonlinear plastic behavior of shear stud is introduced in FE model using a multi-linear isotropic hardening model and Ramberg-Osgood parameters, k' and n' , as shown below:

$$\varepsilon = \frac{\sigma}{E} + \left(\frac{\sigma}{k'}\right)^{n'} \quad (6)$$

The value of K' and n' were obtained from the structural engineering report of Josi and Grondin [10] and were 727 MPa and 0.15 respectively.

3.6 Validation of finite element model

Lee et al. [7] performed push-out tests on three stud diameters of 25, 27 and 30 mm to investigate experimentally static and fatigue behavior of large shear stud connectors. For each diameter of shear stud, three static tests were conducted. Finite element analyses of

these nine specimens were conducted. Details of the validation of static strength of shear stud using FE analysis are presented elsewhere [20]. Table 1 compares the static strengths from push-out tests of Lee et al. [7] with the FE analysis results. A good agreement of both static strength and ultimate slip are found. It is important to note that since three tests were performed for each diameter, the average value was used for comparison purpose. Figure 7 shows that for different stud diameters, the static strength obtained from tests are very close to that obtained from FE analyses.

In addition to Lee et al. [7] test, results from push-out test of Gattesco and Giuriani [17] were compared with results from FE analysis. In their tests, compressive cube strength of concrete (f_{cu}) was used as 32.5 MPa and compressive cylinder strength of concrete was assumed as 26 MPa ($0.8 f_{cu}$). Also, the shear stud diameter for the test was 19 mm. Details of the push-out test of Gattesco and Giuriani [17] are presented elsewhere [20]. Figure 8 presents the finite element model validation of the push-out test of Gattesco and Giuriani [17]. Load versus relative displacement curve from the test was compared with results from FE analysis. The ultimate slip value was reported as 9.7 mm in the test of Gattesco and Giuriani [17], while from FE analysis, it was found as 9.61 mm. The slip at which the load was reduced by 10% from its peak was used as ultimate slip in the developed FE model. The developed FE push-out model was also validated, as shown in Fig. 9, with test results of Loh et al. [21] for 19 mm shear stud. A good correlation of both capacity of shear stud and ultimate slip was observed.

Using the developed finite element model and the proposed approach for fatigue life estimation of headed shear stud connector discussed in the following sections 4.1 and 4.2 fatigue life is estimated for headed shear studs.

4. Prediction of fatigue life

4.1 Crack initiation life

Lee et al. [7] tested 12 specimens for fatigue life investigation on three different diameters: 25, 27 and 30 mm. In this study, five specimens of 25 mm diameter, three specimens of 27 mm and three specimens of 30 mm shear studs were taken and an approach for fatigue life prediction of shear stud using push-out specimen has been proposed. The stress range and concrete strength collected from test of Lee et al. [7] are shown in the following Table 2.

ABAQUS dynamic explicit formulation was adopted for the analysis in this study. ABAQUS explicit formulation has previously been applied in many problems such as crack and failure of concrete material. Dynamic explicit is a time control method since the global mass and stiffness matrices need not be formed and inverted resulting relatively inexpensive increment compared to implicit analysis. It is important to note here that crack was not explicitly modeled in the FE model. Rather, it was assumed that crack will generate in highly stressed area. The location of highly stressed area was identified from FE analysis.

In the first time step, the model was fully loaded to maximum load. The load was then reduced to minimum load in the second time step, and finally it was reloaded to maximum load again in time step 3. After time step 2 and 3, the nominal strains and stress were

recorded from the output file. Lee et al. [7] pointed out the critical location of push-out specimen as the base of the weld collar, which was also observed in FE analysis, shown in Fig.10. Once strain range and maximum stress at critical location were obtained, crack initiation life (N_{init}) was calculated using Eq. (1).

4.2 Crack propagation life

According to the proposed FE based approach, total fatigue life was calculated as summation of crack initiation life and crack propagation life.

Total fatigue life = crack initiation life (N_{init}) + crack propagation life (N_{prop})

Crack propagation life was obtained by integrating Eq. (3) between the limits of initial crack size and final crack size. As started earlier in section 2, for this study, initial crack size of 1 mm was used, and it gave an excellent correlation with test results. For crack propagation life, it is very important to identify the fatigue failure modes. Figure 11 shows the two common fatigue failure modes, Mode A, in which crack initiates at the top of the weld collar and then propagates along the stud-weld interface; in Mode B, crack initiates at the base of the weld collar and propagates until it reaches to the base of the weld collar again through the joist material. In the test of Lee et al. [7], Mode B was reported. Assuming Mode B fatigue failure mode governs final crack size was assumed as weld base diameter. It was pointed out by Josi and Grondin [10] that final crack size has very less effect on the crack propagation life (N_{prop}).

For prediction of crack propagation life, another important parameter is stress intensity factor which is used in fracture mechanics to predict the stress state near the tip of a crack.

The stress intensity factor, K , used in Eq. (3), was calculated using the following formula from the research work of Josi and Grondin [10]:

$$K = \beta_E \beta_S \beta_W \beta_G \sigma \sqrt{\pi a} \quad (7)$$

where $\beta_E, \beta_S, \beta_G, \beta_W$ are correction factors for elliptical crack front, free surface, geometrical discontinuity and finite width respectively. σ is the reference stress in the uncracked condition and a is the half-crack length. The crack shape and stress gradient correction factors were determined using the research work of Ibrahim et al. [14]:

$$\beta_E = \frac{1}{E_K} \quad (8)$$

where E_K = complete elliptical integral of the second kind, and is given by:

$$E_K = \left[1 + 1.464 \left(\frac{a}{b} \right)^{1.65} \right]^{0.5} \quad (9)$$

where a and b are the minor and major semi diameters of an elliptical crack, assuming an elliptical crack shape, respectively. Free surface correction factor, β_S was taken 1.12 as suggested by Broek [22]. The finite thickness correction factor, β_W was determined with the following relationship [22]:

$$\beta_W = \sqrt{\frac{1}{\cos\left(\frac{\pi a}{W}\right)}} \quad (10)$$

β_G was determined using the following formula used by Ibrahim et al. [14]:

$$\beta_G = \frac{SCF}{1 + 0.88a^{0.576}} \quad (11)$$

where SCF is the stress concentration factor. In the research work of Josi and Grondin [10], SCF was taken as 1.0 considering nominal stress, σ at the center of the initial flaw or crack. This assumption was also applied in the present work. The relationship between the two semi-axes of the elliptical crack, a and b proposed by Fisher et al. [13] was employed:

$$b = 1.088 a^{0.946} \quad (12)$$

where a and b are in inches. After getting K , crack propagation life was calculated using Eq. (3).

The fatigue life of the eleven specimens of Lee et al. [7] obtained from FE analyses using the above-mentioned procedure are given below in Table 3. The mean test to predicted (FEA) fatigue life, as shown in Table 3, is 0.996 and the coefficient of variation is 0.41. It is observed from Table 3 that for most of the specimens the proposed FEA based method predicts the fatigue life of headed shear stud reasonably well. For few cases, for specimens FT25A3, FT25B3, and FT30A3, fatigue life from the FEA based approach did not provide very good correlation with test results. This may be due to many factors, such as variability in surface roughness, variability in specimen geometry, weld imperfections, any initial flaws that might cause stress concentrations etc., that affect stresses in shear studs. As an example, FT25A2 and FT25A3 have same geometry and same concrete strength, but stress range applied during the test for FT25A3 specimen is higher (170 MPa) in comparison to FT25A2 (150 MPa). Thus, fatigue life for shear stud specimen FT25A3 should be lower than FT25A2. However, this was not the case in the test and a significant higher fatigue life was reported for the FT25A3 specimen. Since no variability and imperfections were measured for the test specimens, it was not possible to account them in the finite element analysis.

5. Parametric study

With the proposed FE based approach for fatigue life estimation a brief parametric study was conducted to investigate effect of different parameters on fatigue life of shear stud.

Effects of two parameters, stud spacing and concrete compressive strength, on fatigue life of headed shear stud were studied.

5.1 Effect of stud spacing on fatigue life

To investigate the effect of stud spacing on fatigue life, three different shear stud spacings (200 mm, 250 mm, and 300 mm) were considered. In Table 4, FT25A2 and FT25A3 have same concrete compressive strength of 30 MPa and FT25B1 has concrete compressive strength of 40 MPa. In the FE analysis, concrete slab was kept constant (200 mm) for all three specimens. As expected, shown in Table 4, a decrease in the fatigue life was observed with the increase of stud spacing for all fatigue specimens. Figure. 12 shows the variation of fatigue life with the change of stud spacing for fatigue specimen FT25A2.

5.2 Effect of concrete strength on fatigue life of shear stud

From the push-out test of Slutter and Fisher [5] the strength of concrete was found to have minor effects on fatigue life of shear stud. The mean compressive strength of all cylinders was around 30 MPa in their test. Now-a-days, concrete strengths higher than 30 MPa are used in steel-concrete composite bridges. Thus, another parameter, concrete compressive strength was taken to investigate its effects on fatigue life. Five different concrete cylindrical compressive strengths (25, 30, 35, 40 and 45 MPa) were chosen. Results from FE analyses are shown in Table 5 and Fig. 13. It can be observed that an increase in concrete strength leads to an increase in fatigue life.

6. Evaluation of code provisions for fatigue design of shear stud

Bridge Design Codes (CSA S6, 2014; ASSHTO 2014, Eurocode 4) provide guidelines for fatigue design of headed shear studs. This section briefly reviews the fatigue design provisions of shear studs in ASSHTO (2014), Eurocode 4, and CHBDC.

6.1 AASHTO fatigue design provisions

The fatigue design provisions described in the current AASHTO LRFD Bridge Design Specifications (AASHTO 2014) are based on fitting a curve through the test data of Slutter and Fisher [5]. In addition, a constant stress amplitude fatigue limit (CAFL) of 24.2 MPa is provided. AASHTO provides the following equation in terms of the shear force range, Z_r :

$$Z_r = \alpha d^2 \geq 19d^2 \quad (13)$$

where $\alpha = 238 - 29.5 \log N$; d = stud diameter and N = number of fatigue cycles.

Equation (13) can be rearranged as

$$S_r = \frac{4}{\pi} (238 - 29.5 \log N) \geq 24.2 \text{ MPa} \quad (14)$$

Thus, fatigue design curve for stud shear connectors in the AASHTO (2014) is a straight line on a semi-log (S_r -log N) scale.

6.2 Eurocode 4 fatigue design provisions

For welded shear studs used with normal weight concrete, the fatigue curve in Eurocode 4 is given as:

$$(\Delta\tau_R)^m N_R = (\Delta\tau_c)^m N_c \quad (15)$$

where $\Delta\tau_R$ = fatigue shear strength related to the cross-sectional area of the shank of the stud, m = slope of the fatigue strength curve and equal to 8.0, $\Delta\tau_c$ = 90 MPa at a reference value of $N_c = 2 \times 10^6$ cycles, N_R = number of stress-range cycles

Equation (15) can be rearranged in the following log-log equation:

$$\log N = 21.93 - 8 \log S_r \quad (16)$$

Unlike AASHTO, Eurocode 4 does not provide a constant amplitude fatigue limit (CAFL) for shear stud.

6.3 CSA S6-14 fatigue design provisions

Previous edition of CSA S6 (CSA S6-06) had exactly same equations as AASHTO for design of headed shear studs subjected to fatigue loading. These equations were based on pushout test data of Slutter and Fisher [5]. Based on the regression analysis of a large amount of pushout test results by Zhang (2007) changes were made in the fatigue provisions of shear stud in the current edition of CSA S6-14. The current Canadian highway bridge design code (CHBDC), CSA S6-14 adopted a log-log relation between stress range and fatigue life and was approximated by current fatigue category D curve. The detail Category D also has the same constant amplitude fatigue limit (CAFL) of 48 MPa, used in earlier version of S6 (S6-06). This has been retained in the current S6-14. According to current CSA S6-14, shear studs shall be designed to satisfy:

$$\tau_{sr} \leq F_{sr}^D \quad (17)$$

where τ_{sr} is the stress range obtained from analysis; F_{sr}^D is fatigue stress range resistance for Category D, as determined by the following equations.

$$F_{sr}^D = \left(\frac{\gamma}{N_c}\right)^{1/3} \quad (18)$$

$$\text{When } F_{sr} < F_{srt}, F_{sr}^D = \left(\frac{\gamma'}{N_c}\right)^{1/5} \geq \frac{F_{srt}}{2} \quad (19)$$

where γ, γ' are fatigue life constants pertaining to the fatigue detail category D; N_c is specified number of design stress cycles.

The reason for using a fatigue curve with two slopes is an approximate way to take into account the progressive reduction of the CAFL because of the damage caused by the stress ranges higher than CAFL. Fracture mechanics also confirms this reduction of the slope of the S-N curve in the high cycle fatigue region.

6.4 Regression analysis of pushout test data

An analysis of the log of stress range (S_r , MPa) and log of fatigue life (N) obtained from push-out tests presented in literature (Lehman et al. [23]; Slutter and Fisher [5]; Mainstone and Menzies [24]; Hallam [25]; Roderick and Ansorian [26]; Lo [27]; Oehlers and Foley [28]; Maeda and Matsui [29]; Naithani et al. [30]; Oehlers [31]; Faust et al. [32]; Bode et al. [33]; Shim et al. [34]; Badie et al. [35]; Lee et al. [7]; Ahn et al. [36]; Hanswille et al. [37]; Mundie [8]) was conducted to evaluate the current fatigue curves in bridge codes. In total, 344 push-out test results were used in the regression analysis. The mean regression line for push-out tests data is represented in the form of:

$$\log N = m \cdot \log S_r + \log a \quad (20)$$

It is common practice to take the design equation as the mean minus two standard deviations, which can be expressed as:

$$\log N = m \cdot \log S_r + \log a - 2\sigma \quad (21)$$

where σ is the standard deviation = $\sqrt{\frac{\sum_{i=1}^n (\text{predicted} - \text{measured})^2}{n-2}}$

m and a are regression constants, representing the slope and intercept of the regression line; n is the number of test data points.

Results from regression analysis of all the pushout test data are shown in Table 6. The linear log-log design curve was obtained by shifting the mean regression line by 2 times the standard deviation. Figure 14 presents the regression lines for the selected pushout tests. Both mean and the design (mean-2 σ), regression lines are presented. The regression lines were constrained to have a slope 3.0. This is because the slope constant 3 has been a best fit for a large number of different structural details tested in fatigue. The regression lines were also compared against the current Canadian fatigue category design curves. It is observed that the design regression line lies above the design curve for fatigue Category E1. The mean regression line closely matches with current Canadian fatigue curve for fatigue category D. The linear log-log mean regression curve is in good agreement with the previous Canadian fatigue curve in the infinite life region, when the number of cycles is more than approximately 1 million.

Results from regression analysis were also compared, as shown in Fig. 15, with the fatigue design curves in different codes. Since the AASHTO/CSA S6-06 fatigue design curve for shear stud curve is semi-log, the fatigue design stress range decreases more rapidly in the

high cycle fatigue region (when the number of cycles is more than 1 million). In comparison to Eurocode, AASHTO/ CSA S6-06 fatigue design curve for shear stud is always conservative.

Badie et al. [35] and Mundie [8] conducted pushout tests with shear stud diameters of 22.2 mm and 31.8 mm. A comparison of the mean regression line of fatigue test results of 31.8 mm diameter studs (25 push-out test data) with 22 mm diameter studs (23 push-out test data) indicates, as shown in Fig. 16, that there is no significant difference of fatigue resistance between the two diameters.

6.5 Evaluation of CAFL for headed shear stud

Unlike Eurocode, both AASHTO and Canadian Highway Bridge design code (CHBDC), CSA S6-14 have included a constant amplitude fatigue limit of 48 MPa for shear stud which often governs the stud fatigue design for bridges with moderate-to-high traffic demands. However, no reference has been cited to justify this CAFL value. In this section, available fatigue test results near the existing CSA/AASHTO CAFL will be reviewed to evaluate the CAFL value for shear stud. In general, the highest stress range at which a runout (non-failure) occurs can be considered as the constant amplitude fatigue threshold. In this study, push-out fatigue tests performed at applied stress levels ranging in values from 30 MPa to 100 MPa and declared as runouts are considered. Both double sided and single sided pushout test results with 3/4 inch and 7/8 inch shear studs are considered. In addition, the FE based approach proposed in this paper is used to analyses fifteen (15) more cases where the push-out specimens were subjected to stress ranges between 40 MPa and

100 MPa. Three different stud diameters (19 mm, 25 mm, and 27 mm) were considered in analysis. Table 7 presents the details of the selected specimens and estimated fatigue life for the shear studs.

It can be seen from Fig. 17 that most of the runout test data are close to the current CAFL value of 48 MPa. The mean value of stress ranges at which runout occurs are 56 MPa and 70 MPa for 3/4 inch and 7/8 inch shear studs, respectively. In Europe, often, the stress cycle corresponding to 5 million cycles is set as the constant amplitude limit for that detail. From Fig. 17, the stress range corresponding to 5 million cycles from CHBDC fatigue curve is about 52 MPa. Thus, current CAFL value of 48 MPa in CSA S6-14 and AASHTO 2014 appears to be conservative.

7. Summary and Conclusions

A finite element based approach using the push-out test is proposed for fatigue life estimation of headed shear stud connectors. Both crack initiation life and crack propagation life were estimated and a good correlation was found with test results. The finite element model using the proposed approach was used to conduct a parametric study to investigate the effect of concrete strength and stud spacing on fatigue life of shear stud. In addition, a regression analysis of the push-out test data available in literature was conducted. The following conclusions were drawn from this study.

- (1) From the regression analysis, it can be observed that the mean regression line could be closely approximated by the fatigue Category D curve of Canadian highway

- bridge design code (CHBDC). Considering that pushout test results provides lower bound estimation of fatigue life of shear studs a mean regression line is justified to use. In addition, the proposed fatigue curve in current CHBDC is still conservative, especially in the high cycle fatigue region where most of the bridges will fall.
- (2) Regression analysis of push-out test data showed that AASHTO provides the most conservative estimate of fatigue life of shear stud both in high cycle fatigue and low cycle fatigue regions in comparison to Eurocode and Canadian standard. In addition, notable amount of overestimation of fatigue life was observed in case of CSA S6-14 in the low cycle fatigue region.
 - (3) A closer look at the run-out test results from pushout tests showed that the current constant amplitude fatigue threshold of 48 MPa is reasonable value to use. With more test results available near the stress range of CAFL, the limiting CAFL value can be increased.
 - (4) Study showed that the current fatigue curves in codes can be used for shear stud of diameter of 31.8 mm. Thus, restriction of use of studs larger than 25 mm (1 inch) in different bridge codes (CSA S6, Eurocode 4, and AASHTO) can be waived.
 - (5) The parametric study revealed that the effect of concrete strength on fatigue life is insignificant. Also, fatigue life decreases with the increase of shear stud spacing for all fatigue specimens.

Acknowledgements

Funding for this research project is provided by the Faculty of Engineering and Computer Science, Concordia University, Montreal, Canada, and the Natural Sciences and

Engineering Research Council of Canada. The authors also gratefully acknowledge Dr. Gilbert Y Grondin of AECOM, Edmonton, AB, Canada for his valuable suggestions in this project.

LIST OF SYMBOLS

$\frac{\Delta\varepsilon}{2}$	Strain amplitude
σ'_f	Fatigue strength coefficient
N_{init}	Crack initiation life
σ_{max}	Maximum applied stress
E	Elastic modulus
b	Fatigue strength exponent
ε'_f	Fatigue ductility coefficient
c	Fatigue ductility exponent
da/dN	Crack growth rate
ΔK	Stress intensity factor range
C	Fatigue constant
m	Slope of the design curve
N_{prop}	Crack propagation life
a_o	Initial crack size
a_f	Final crack size
ΔK_{th}	Threshold stress intensity factor range
$E_{concrete}$	Elastic modulus of concrete
f'_c	Concrete compressive strength

f_t	Concrete tensile strength
K	Stress intensity factor
$\alpha\epsilon_{c1}$	Ultimate strain of concrete
$\beta\epsilon_t$	Tensile strain at zero stress
ϵ_{c1}	Compressive strain of concrete
ϵ_t	Tensile strain of concrete
β_E	Correction factor for elliptical crack front
β_s	Correction factor for free surface
β_G	Correction factor for geometrical discontinuity
β_W	Correction factor for finite width
a	minor semi diameter of an elliptical crack, or half the crack length
b	major semi diameter of an elliptical crack
E_K	Complete elliptical integral of the second kind
SCF	Stress concentration factor
Z_r	Shear force range
d	Shear stud diameter
N	Number of fatigue cycles
S_r	Stress range
$\Delta\tau_R$	Stress range
N_R	Number of stress range cycles
$\Delta\tau_c$	Reference stress range
N_c	Specified number of design stress cycles
τ_{sr}	Stress range
F_{sr}^D	Fatigue stress range resistance for category D
γ	Fatigue life constant to fatigue detail category D
γ'	Fatigue life constant to fatigue detail category D
F_{srt}	Threshold stress range

References

- [1] CAN/CSA S6-14. Canadian Highway Bridge Design Code, Toronto, Ontario, Canada; 2014.
- [2] AASHTO LRFD Bridge Design Specifications. American Association of State Highway and Transportation Officials, Washington, D.C; 2014
- [3] CEN 1994-2 Eurocode 4. Design of composite steel and concrete structures - Part 2: General rules for bridges. Brussels, Belgium; 2005.
- [4] CAN/CSA S6-06. Canadian Highway Bridge Design Code, Toronto, Ontario, Canada; 2014.
- [5] Slutter, R.G., and Fisher, J.W. Fatigue strength of shear connectors. Highway research record no. 147, National Research Council, Washington, D.C; 1966.
- [6] ABAQUS standard user's manual, Version 6.13. Hibbitt, Karlsson and Sorensen, USA; 2013.
- [7] Lee, P.G., Shim, C.S., and Chang, S.P. Static and fatigue behavior of large stud shear connectors for steel-concrete composite bridges. Journal of Constructional Steel Research 2005; 61(9): 1270-1285.
- [8] Mundie, D.L. Fatigue testing and design of large diameter shear studs used in highway bridges. M.Sc. thesis. Department of Civil Engineering, Auburn University, USA; 2011.
- [9] Smith, K.N, Watson, P., and Topper, T.H. A stress-strain function for the fatigue of materials. Journal of Materials 1970; 5(4): 767-778.

- [10] Josi, G., and Grondin, G.Y. Reliability-based management of fatigue failures. Structural Engineering Report 285, Department of Civil and Environmental Engineering, University of Alberta, Edmonton, Canada; 2010.
- [11] Paris, P., and Erdogan, F. A critical analysis of crack propagation laws. *Journal of Basic Engineering* 1963; 85(4): 528-533.
- [12] ASTM designation E647. Standard test method for measurement of fatigue crack growth rates, American Society for Testing and Materials. Philadelphia, USA; 2000.
- [13] Fisher, J.W., Albrecht, P.A., Yen, B.T., Klingerman, D.J., and McNamee, B.M. Fatigue strength of steel beams with welded stiffeners and attachments. NCHRP report no. 147, Transportation Research Board, National Research Council, Washington, D.C; 1974.
- [14] Ibrahim, S.A., El-Dakhkhni, W.W., Elgaaly, M. Fatigue of corrugated-web plate girders: Analytical study. *Journal of Structural Engineering* 2006; 132(9): 1381-1392.
- [15] Ellyin, F. Fatigue damage, crack growth and life prediction. Chapman & Hall, London, U.K; 1997.
- [16] Chen, H., Grondin, G.Y., and Driver, R.G. Fatigue resistance of high performance steel. Structural Engineering Report 258, Department of Civil and Environmental Engineering, University of Alberta, Edmonton, Canada; 2005.
- [17] Gattesco, N. and Giuriani, E. Experimental study on stud shear connectors subjected to cyclic loading. *Journal of Constructional Steel Research* 1996; 38(1): 1-21.
- [18] CAN/CSA-A23.3-14. Design of concrete structures, Toronto, Ontario, Canada; 2014.

- [19] Ellobody, E., Young, B., Lam, D. Behavior of normal and high strength concrete-filled compact steel tube circular stub columns. *Journal of Constructional Steel Research* 2006; 62(7): 706-715.
- [20] Mia, M. M., Bhowmick, A.K. Static Strength of Headed Shear Stud Connectors Using Finite Element Analysis. 6th International Conference on Engineering Mechanics and Materials 2017, Vancouver, BC, Canada, May 31-June 3.
- [21] Loh, H.Y., Uy, B. and Bradford, M.A. The effects of partial shear connection in the hogging moment regions of composite beams, Part I – Experimental study. *Journal of Constructional Steel Research* 2004; 60: 921-62.
- [22] Broek, D. The practical use of fracture mechanics. 2nd ed. Kluwer Academic Publishers, Netherlands; 1989.
- [23] Lehman, H. G., Lew, H.S., and Toprac, A.A. Fatigue strength of 3/4 inch studs in lightweight concrete. Research Report No. 76-1F, Center for Highway Research, The University of Texas, Austin, Texas; 1965.
- [24] Mainstone, R. J. and Menzies, J.B. Shear Connectors in Steel Concrete Composite Beams for Bridges 1: Static and Fatigue Test on Push-out Specimens. *Concrete* 1967; 291-302.
- [25] Hallam, M. W. The behaviour of stud shear connectors under repeated loading. Research Report No, R281, University of Sydney, School of Civil Engineering, Sydney, Australia; 1976.
- [26] Roderick, J. W., and Ansorian, P. Repeated loading of composite beams. *Civil Engineering Transactions* CE18(2) 1976;109-116.

- [27] Lo KK. Fatigue testing of stud shear connectors. M.Eng thesis, University of Melbourne, 1978.
- [28] Oehlers DJ, Foley L. The fatigue strength of stud shear connectors in composite beams. Proc. Instn Civ. Engrs, Part 2, 79, 349–364, 1985.
- [29] Maeda Y and Matsui S. Effects of concrete placing direction on static and fatigue strengths of stud shear connectors. Tech. Reports, Osaka University, October 1983; 33(1733):397–406.
- [30] Naithani, K.C., Gupta, V.K. and Gadh, A.D. Behavior of Shear Connectors under Dynamic Loads. Materials and Structures 1988; 21 (125): 359-363.
- [31] Oehlers, D. J. The Derivation of the Fatigue Endurance of Stud Shear Connections in Composite Steel and Concrete Bridge Beam. Department of Civil Engineering. The University of Adelaide. Report No. R81, 1988.
- [32] Faust, T., Leffer, A., and Mensinger, M. Fatigue of Headed Studs Embedded in LWAC. LACER No. 4, 1999; 226-230.
- [33] Bode, H., Mensinger, M, and Leffer, A. The Shear Connection of Steel-Concrete Composite Bridges under Non-Static Loading. Stahlbau, 2001; 70 (4): 277-286.
- [34] Shim, C.S., Lee, P.G. and Chang, S.P. Design of Shear Connection in Composite Steel and Concrete Bridges with Pre-Cast Decks. Journal of Constructional Steel Research 2001, 57(2): 203-219.
- [35] Badie, S.S. Tadros, M.K., Kakish, H.F., Splittgerber, D.L. and Baishya, M.C. Large Shear Studs for Composite Action in Steel Bridge Girders. Journal of Bridge Engineering 2002; 7(3):195-203.

- [36] Ahn, J. H., Kim, S. H., and Jeong, Y. J. Fatigue experiment of stud welded on steel plate for a new bridge deck system. *Steel and Composite Structures* 2007; 7(5): 391-404.
- [37] Hanswille, G., Porsch, M., and Ustundag, C. Resistance of headed studs subjected to fatigue loading Part I: Experimental study. *Journal of Constructional Steel Research* 2007; 63(4): 475-484.

ACCEPTED MANUSCRIPT

Table 1: Comparison of FE Analysis Results with Test Results of Lee et al. [7]

Diameter of Stud (mm)	Test Results				FE Analysis Results		
	Specimen	Staic strength (kN)	Average	Ultimate slip (mm)	Average	Staic strength (kN)	Ultimate slip (mm)
25	ST25B1	176.4		6.33			
	ST25B2	176.7	180.13	6.72	6.79	175.39	8.59
	ST25B3	187.3		7.31			
27	ST27C1	208.2		9.19			
	ST27C2	238.5	211.20	8.36	8.82	208.00	9.12
	ST27C3	186.9		8.92			
30	ST30C1	222.8		9.39			
	ST30C2	240.0	232.27	9.24	9.36	242.92	10.02
	ST30C3	234.0		9.46			

Table 2. Selected specimens for FE analysis

Specimen	Concrete strength (MPa)	Stress range (MPa)
FT25A2	30	150.0
FT25A3	30	170.0
FT25B1	40	130.0
FT25B2	40	150.0
FT25B3	40	177.3
FT27A1	30	128.4
FT27A2	30	150.0
FT27A3	30	170.0
FT30A1	30	130.0
FT30A2	30	150.0
FT30A3	30	156.1

Table 3. Fatigue life prediction by the proposed approach

Specimen	Fatigue life (Test)	Fatigue life (FEA)	Variation (Test/FEA)
FT25A2	44827	50586	0.886
FT25A3	60000	38646	1.553
FT25B1	387209	355439	1.089
FT25B2	61063	61351	0.995
FT25B3	5320	29409	0.181
FT27A1	142641	135513	1.053
FT27A2	22488	26797	0.839
FT27A3	13766	20752	0.663
FT30A1	75484	55897	1.350
FT30A2	10436	13453	0.776
FT30A3	19333	12331	1.568
Mean of Test/FEA			0.996
COV of Test/FEA			0.41

Table 4. Fatigue life variation with stud spacing

Stud spacing (mm)	Fatigue life (cycles)		
	FT25A2	FT25A3	FT25B1
200	134360	89275	376015
250	50586	38646	355439
300	22545	17143	231393

Table 5. Fatigue life variation with concrete strength

Concrete strength (MPa)	Fatigue life (cycles)		
	FT25A2	FT25A3	FT25B1
25	41478	32919	296636
30	50586	38646	309500
35	55608	47197	318768
40	61351	66031	355439
45	62184	69791	450018

Table 6. Regression analysis of pushout test data

Constant	Regression value	Constrained regression value
m	3.432	3.0
$\log a_{mean}$	12.684	11.773
$\log a_{design}$	11.46	10.32
a_{mean}	4.83×10^{12} MPa	5.93×10^{11} MPa
a_{design}	2.88×10^{11} MPa	2.09×10^{10} MPa

Table 7. Selected cases for CAFL evaluations

Specimen	Stress range (MPa)	Fatigue life (FEA)
FT19	40	25755000
FT19	50	15782000
FT19	60	11795000
FT19	70	8945200
FT19	80	6955000
FT19	100	3459650
FT25	40	14155700
FT25	50	10542450
FT25	60	7150000
FT25	70	6255000
FT25	80	5450000
FT25	100	1310000
FT27	60	4193000
FT27	80	1887936
FT27	100	969300

Figure Captions for “A finite element based approach for fatigue life prediction of headed shear studs”

Md. Manik Mia and Anjan K. Bhowmick

Department of Building, Civil and Environmental Engineering, Concordia University,
Montreal, Quebec, Canada

Fig. 1. Push-out specimen: (a) Geometry of pushout test of Lee et al. [7]; and
(b) A quarter of push-out specimen used in FE model

Fig. 2. Surfaces in contact interaction between steel beam and concrete slab

Fig.3. MPC constraint between load surface and control constraint point

Fig. 4. Boundary condition for finite element model

Fig. 5. FE mesh of the Model: (a) Concrete slab, (b) Steel beam with stud, and (c) Shear stud with weld

Fig. 6. Stress-strain relationships for concrete material

Fig. 7. Validation of FE model with test results of Lee et al. [7]

Fig. 8. Validation of FE model with test results of Gattesco and Giuriani [17]

Fig. 9. Validation of FE model with test results of Loh et al. [21]

Fig. 10. Critical location of shear stud

Fig. 11. Fatigue failure modes: (a) Mode A; and (b) Mode B

Fig. 12 Effect of stud spacing on fatigue life (FT25A2)

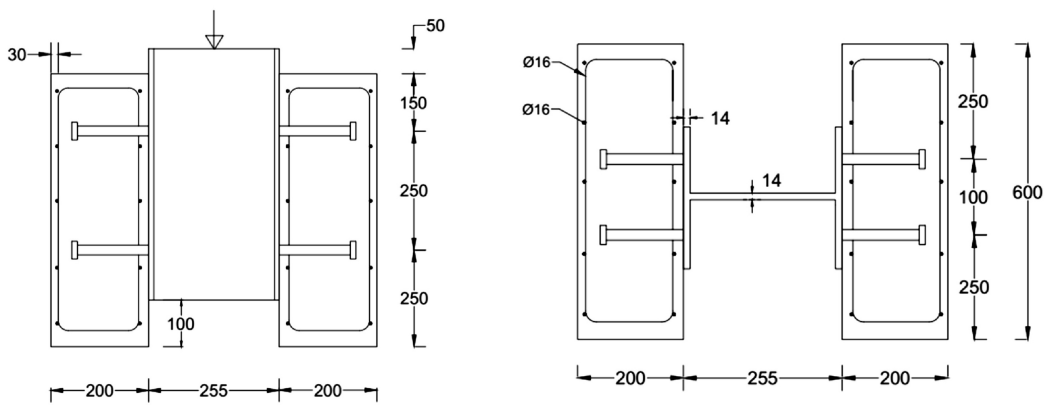
Fig. 13. Concrete strength effects on fatigue life of shear studs (FT25A2)

Fig. 14. Regression analysis of push-out test data

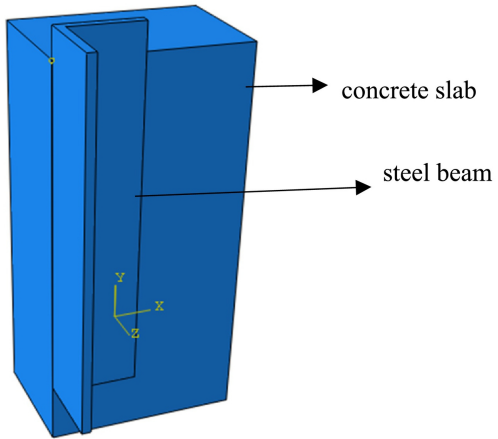
Fig. 15. Evaluation of fatigue curves in different codes

Fig. 16. Regression analysis of push-out test by Badie et al. [34] and Mundie [8]

Fig. 17. Current design curves with available run-out test data



(a)



(b)

Figure 1

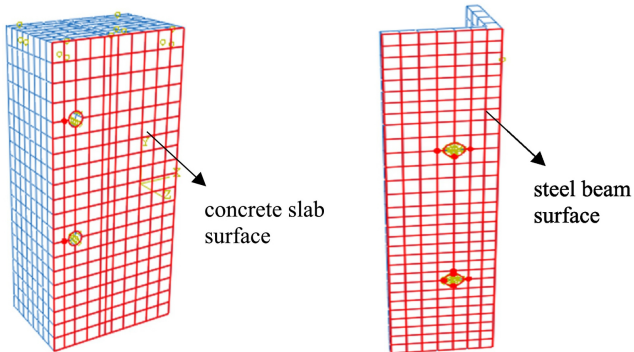


Figure 2

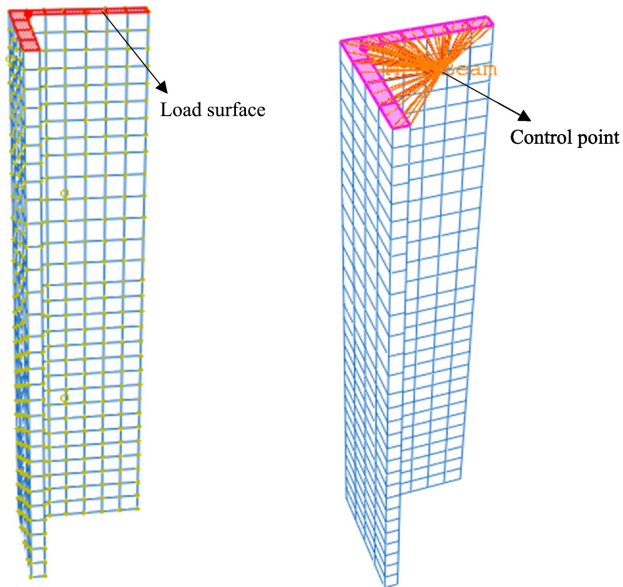
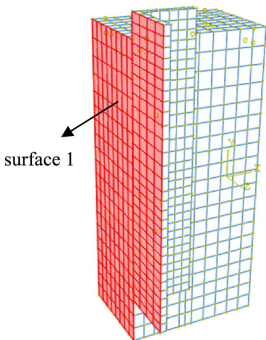
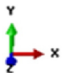
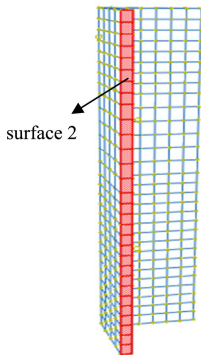


Figure 3

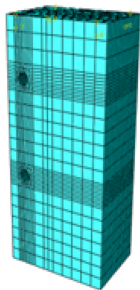


a) X-axis symmetric boundary condition

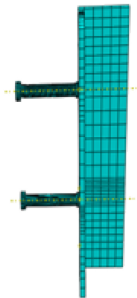


b) Z-axis symmetric boundary condition

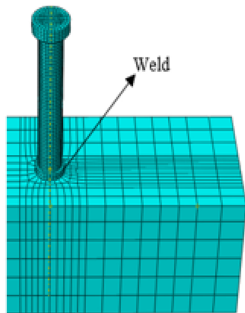
Figure 4



a)



b)



c)

Figure 5

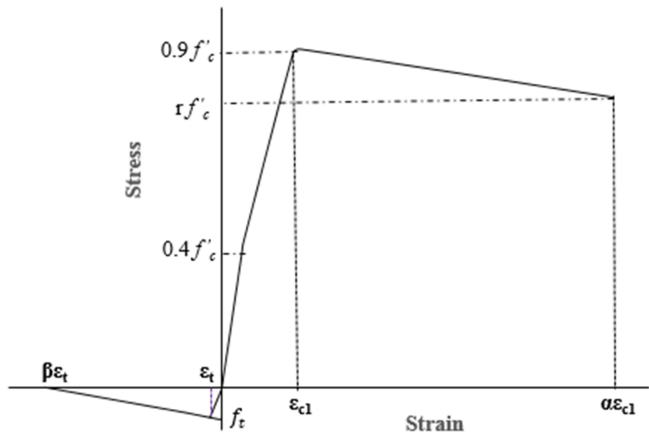


Figure 6

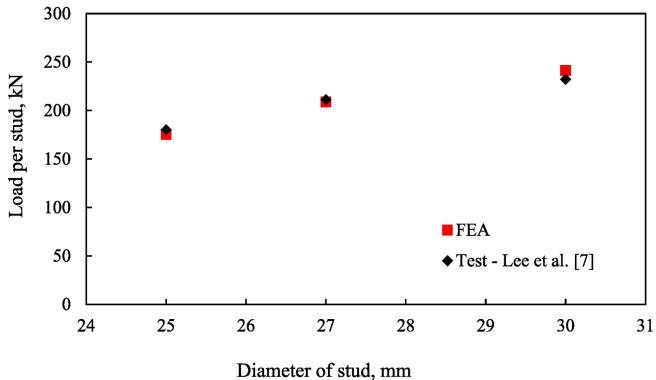


Figure 7

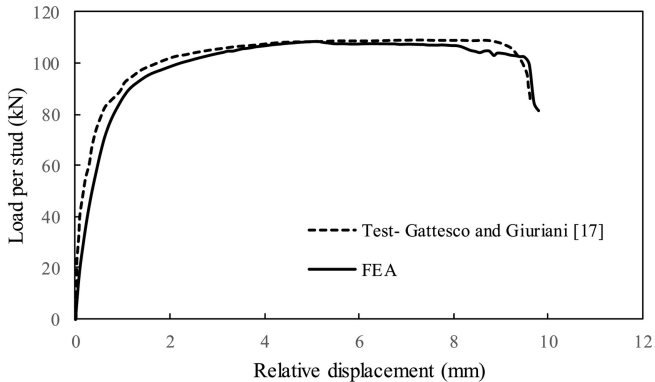


Figure 8

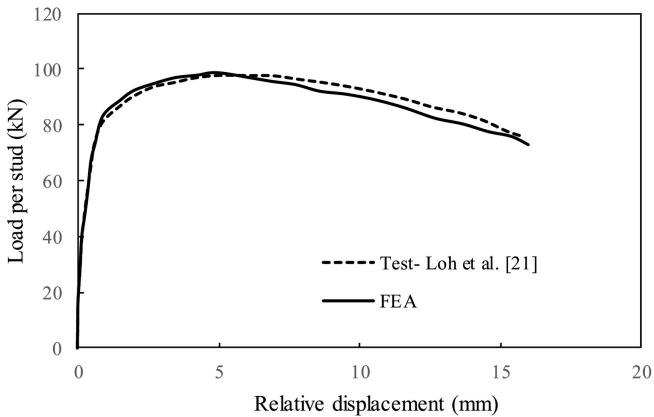


Figure 9

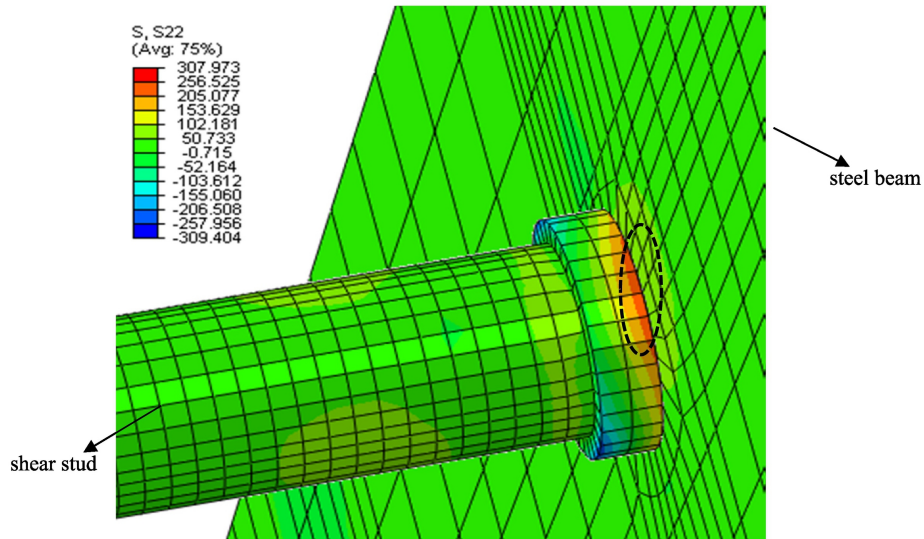
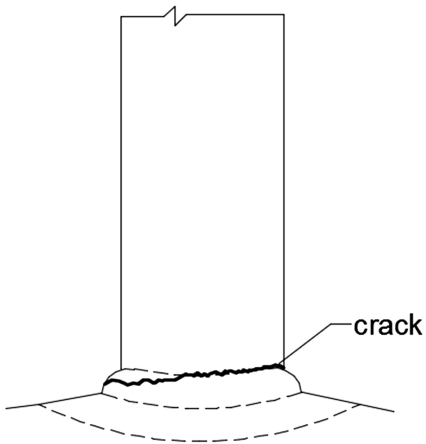


Figure 10

(a)



(b)

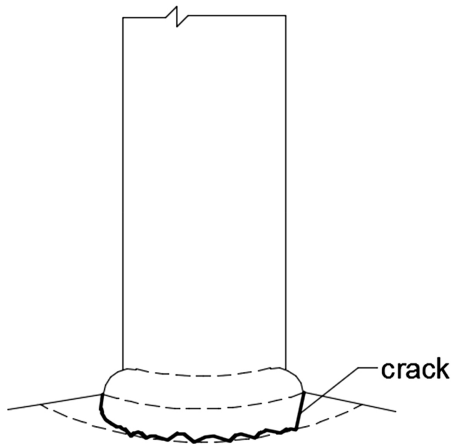


Figure 11

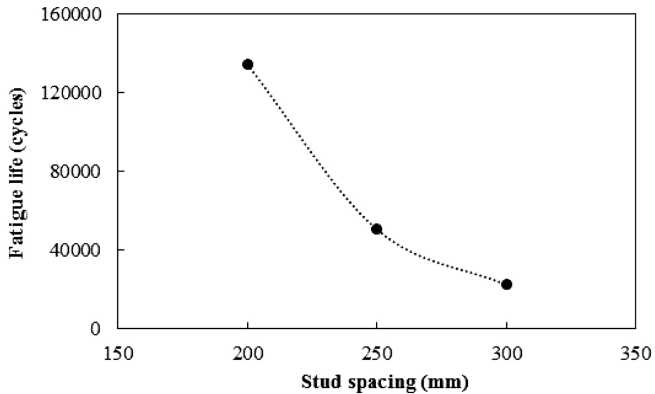


Figure 12

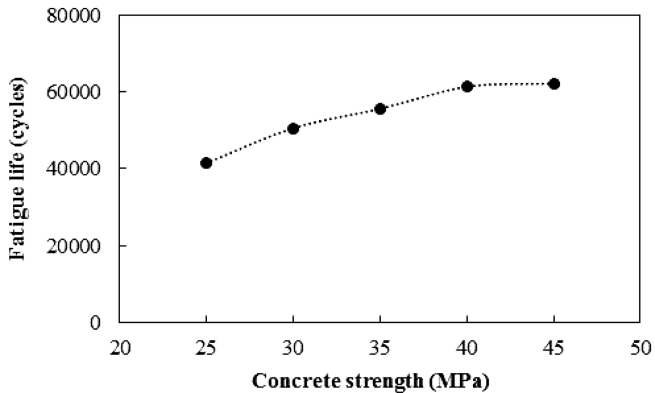


Figure 13

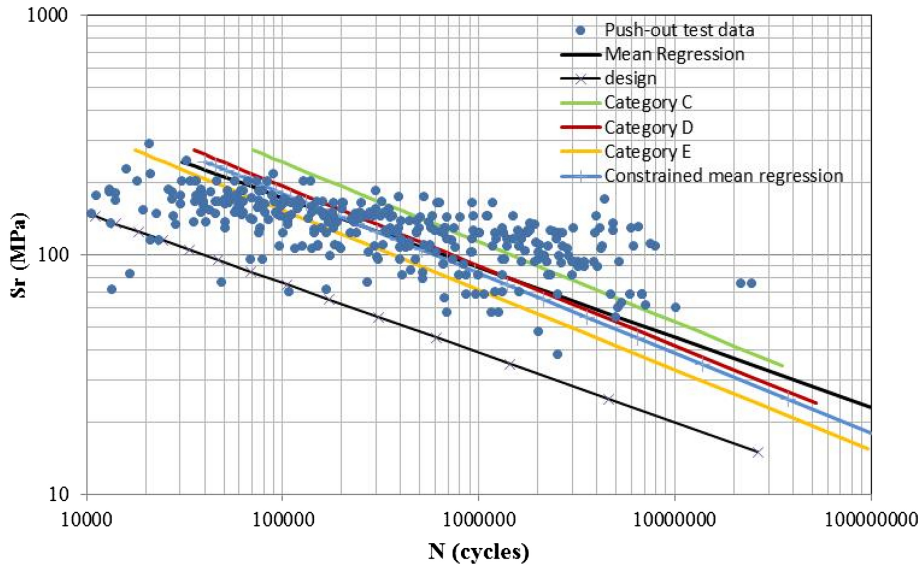


Figure 14

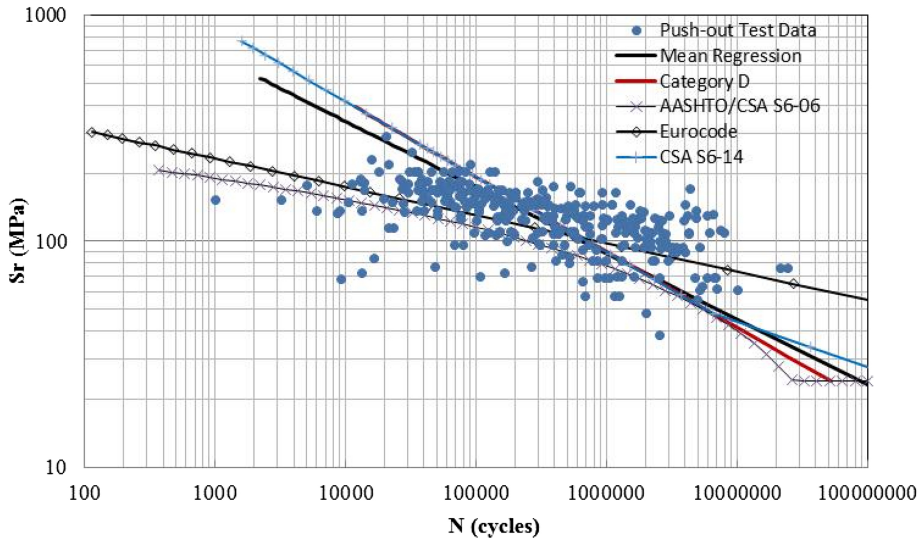


Figure 15

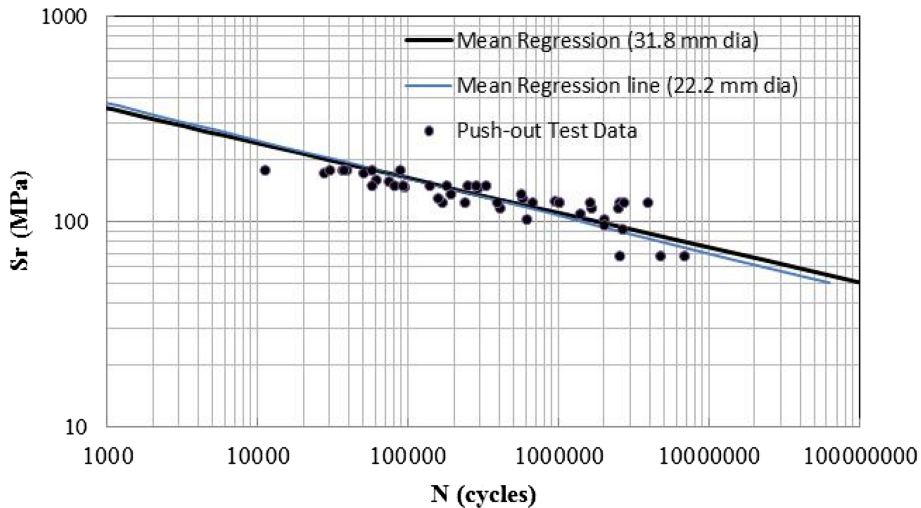


Figure 16

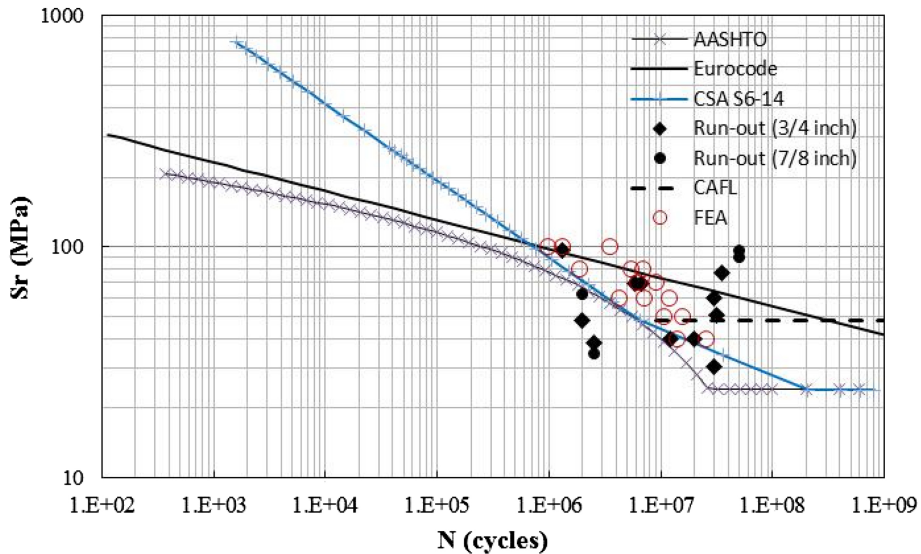


Figure 17